AGU PUBLICATIONS

JGR

Journal of Geophysical Research: Solid Earth

RESEARCH ARTICLE
10.1002/2013JB010597

Key Points:
- The maximum magnitude of earthquakes induced by fluid injection can be capped
- The upper-bound seismic moment is proportional to the volume of injected fluid
- The largest fluid-induced earthquakes are caused by deep injection of wastewater

Correspondence to:
A. McGarr,
mcgarr@usgs.gov

Citation:
McGarr, A. (2014), Maximum magnitude earthquakes induced by fluid injection, *J. Geophys. Res. Solid Earth*, *119*, 1008–1019, doi:10.1002/2013JB010597.

Received 12 AUG 2013
Accepted 3 JAN 2014
Accepted article online 8 JAN 2014
Published online 4 FEB 2014

Maximum magnitude earthquakes induced by fluid injection

A. McGarr[1]

[1]United States Geological Survey, Menlo Park, California, USA

Abstract Analysis of numerous case histories of earthquake sequences induced by fluid injection at depth reveals that the maximum magnitude appears to be limited according to the total volume of fluid injected. Similarly, the maximum seismic moment seems to have an upper bound proportional to the total volume of injected fluid. Activities involving fluid injection include (1) hydraulic fracturing of shale formations or coal seams to extract gas and oil, (2) disposal of wastewater from these gas and oil activities by injection into deep aquifers, and (3) the development of enhanced geothermal systems by injecting water into hot, low-permeability rock. Of these three operations, wastewater disposal is observed to be associated with the largest earthquakes, with maximum magnitudes sometimes exceeding 5. To estimate the maximum earthquake that could be induced by a given fluid injection project, the rock mass is assumed to be fully saturated, brittle, to respond to injection with a sequence of earthquakes localized to the region weakened by the pore pressure increase of the injection operation and to have a Gutenberg-Richter magnitude distribution with a *b* value of 1. If these assumptions correctly describe the circumstances of the largest earthquake, then the maximum seismic moment is limited to the volume of injected liquid times the modulus of rigidity. Observations from the available case histories of earthquakes induced by fluid injection are consistent with this bound on seismic moment. In view of the uncertainties in this analysis, however, this should not be regarded as an absolute physical limit.

1. Introduction

The modern oil and gas boom, often involving production from unconventional reservoirs, has led to a measurable increase in earthquakes large enough to add significantly to the seismic hazard, at least in the central and eastern United States [*National Research Council*, 2013]. Of the seven main shocks of magnitude (*M*) 4, or greater, that occurred east of the Rocky Mountains during 2011, six are reported to have been induced by activities associated with oil and gas production; the only natural earthquake, according to the reports, was the *M*5.8 event near Mineral, Virginia: (1) *27 February M4.7 Guy*, *Arkansas* (Wastewater injection [*Horton*, 2012]); (2) *23 August M5.3 Trinidad*, *Colorado* (Wastewater injection; J. L. Rubinstein et al., manuscript submitted for publication, 2013); (3) *23 August M5.8 Mineral Virginia* (Natural [*Chapman*, 2013]); (4) *11 September M4.3 Cogdell*, *Texas* (Fluid injection for enhanced oil recovery [*Davis and Pennington*, 1989; *Gan and Frohlich*, 2013]); (5) *20 October M4.8 South Texas* (Conventional natural gas production from Fashing field [*Pennington et al*., 1986; *Frohlich and Brunt*, 2013]); (6) *6 November M5.7 Prague*, *Oklahoma* ("Potentially induced by wastewater injection" according to [*Keranen et al*., 2013]); and (7) *31 December M4 Youngstown Ohio* (Wastewater injection [*Ohio Department of Natural Resources*, 2012; *Kim*, 2013]).

As oil and gas production from unconventional reservoirs expands, it seems likely that the occurrence of induced earthquakes associated with these activities will also increase. Accordingly, there is a need to understand how these anthropogenic earthquakes are induced and the extent to which they augment the earthquake hazard, especially in the central and eastern United States where much of the modern oil and gas boom is occurring and where the natural level of seismicity is relatively low.

From unconventional reservoirs, gas or oil is typically produced from a low-permeability formation (e.g., Marcellus shale) by injecting fluid under pressure to either propagate cracks through the rock (hydraulic fracture) or to stimulate slip across preexisting faults (hydroshear) to enhance permeability and allow gas or oil to flow more readily into the well bore. These permeability-enhancing treatments induce earthquakes, but, with only a few exceptions, the microearthquakes have been too small to be felt at the surface; exceptions were reported by *Holland* [2013], *De Pater and Baisch* [2011], and *BC Oil and Gas Commission* [2012].

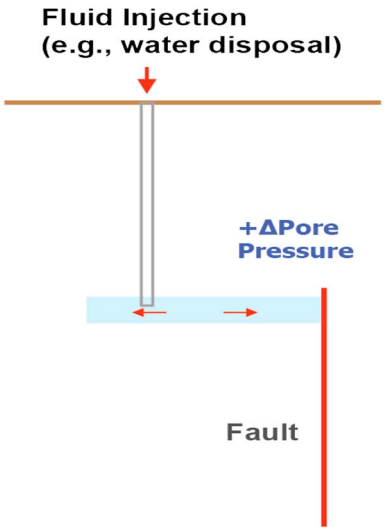

Figure 1. Wastewater is injected into a deep aquifer that hydraulically transmits increased pore pressure to a nearby fault. The increase of pore pressure in the fault zone reduces the effective normal stress acting on the fault, thereby reducing the fault strength and promoting earthquake slip. (adapted from *McGarr et al.* [2002, Figure 1]).

Along with the oil and gas produced from unconventional reservoirs, there are considerable quantities of coproduced wastewater, which consists of fluids injected to enhance permeability as well as formation brines. This wastewater is commonly injected deep underground for disposal.

At the outset, it is important to note that only a tiny fraction of the approximately 30,000 Class II wastewater disposal wells used to inject waste fluids from oil and gas activities into undepleted formations induce earthquakes large enough to be felt. Despite the low probability that a particular wastewater injection well will cause felt earthquakes, there are so many of these wells that this source of earthquakes evidently adds significantly to the total seismic hazard, at least in the central and eastern United States [e.g., *Ellsworth*, 2013].

Ideally, it would be useful to be able to predict in advance of a planned injection activity whether there will be induced seismicity of any consequence. For instance, perhaps the magnitude distribution of the induced earthquakes could be forecast based on various factors including the fluid injection parameters and the rheologies of the geologic formations in the vicinity of the injection interval. Currently, however, our understanding of how, or whether, a given injection activity induces earthquakes is inadequate to make this sort of prediction, beyond having a general sense of the factors that seem to favor a significant seismic response.

Frohlich [2012] proposed that fluid injection triggers earthquakes if pore pressure increase is transmitted to a nearby fault that is suitably oriented for slip in the ambient stress field. The scenario illustrated schematically in Figure 1 appears to describe some of the case histories for which injection of wastewater led to sequences of induced earthquakes. That is, injection into a deep aquifer raises the pore pressure, which is hydraulically communicated from the injection interval along the aquifer to a nearby buried fault that extends into the crystalline basement [e.g., *Horton*, 2012]. The elevated pore pressure in the fault zone reduces the effective normal stress resulting in earthquake fault slip [*Hubbert and Rubey*, 1959]. Alternatively, injection directly into the crystalline basement [e.g., *Healy et al.*, 1968] appears to be especially effective for the generation of earthquakes large enough to be felt [*Kim*, 2013]. In general, it seems that injection leading to pore pressure increase within a seismogenic rock mass is a necessary condition for inducing earthquakes.

The concept that pore pressure increase due to fluid injection can stimulate fault slip is well established [e.g., *Hubbert and Rubey*, 1959; *Healy et al.*, 1968; *Raleigh et al.*, 1976]. This raises the question, however, of how large can the magnitudes of the earthquakes induced by the increase in pore pressure be?

Evidence is presented here that suggests that the maximum seismic moment M_0 or magnitude for a specified injection activity may be limited according to the total volume of fluid injected during the time leading up to the largest earthquake. This implied upper bound can be understood in terms of how a seismogenic, saturated rock mass is expected to respond to the injection of liquid, as will be described.

This study was motivated partly by the need to update results reported by *McGarr* [1976] who argued for a relation between induced volume changes, positive or negative, of various activities, such as mining or fluid injection at depth, and the cumulative seismic moment. This report focuses on fluid injection and revises the previous results.

2. Maximum Seismic Moment Versus Injected Volume

Figure 2 and Table 1 show the maximum seismic moment as functions of the total volume of liquid injected up to the time of the largest induced earthquake. For most of the case histories represented here, the injection is

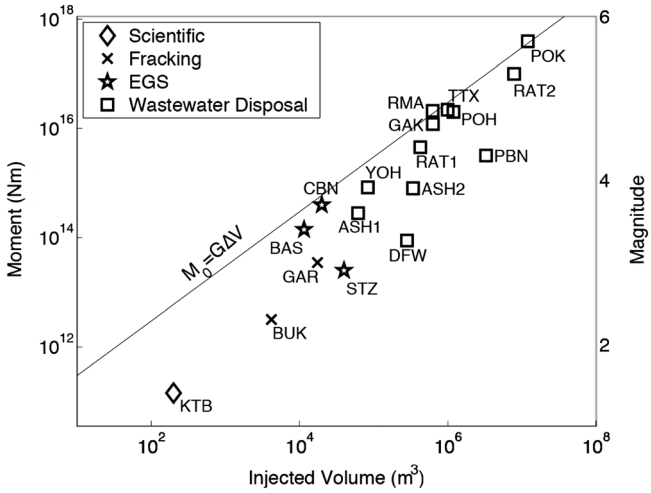

Figure 2. Maximum seismic moment and magnitude as functions of total volume of injected fluid from the start of injection until the time of the largest induced earthquake. The equation along the solid line relates the upper bound seismic moment to the product of the modulus of rigidity and the total volume of injected fluid. These data are listed in Table 1.

either down a single well or down several wells near to each other and so the relation between the injection activity and the resulting earthquakes is usually straightforward. For several of the case histories, however, injection wells in different locations in the epicentral area of an earthquake sequence may have contributed to the pore pressure increases responsible for the earthquakes; these cases are more challenging owing to uncertainties concerning hydrological conditions that might influence pore pressure changes in the fault zones. In this study, an important criterion for deciding whether a particular well played a role in causing the earthquake sequence has been the spatial relationship of the earthquake locations to the well [e.g., *Hsieh and Bredehoeft*, 1981]; that is, a well is considered to have contributed to the pore pressure increase that caused the sequence if the locations of some of the earthquakes indicate a likely relationship to fluid injection.

Among the activities involving the injection of fluids at depth that can induce earthquakes, the four represented in Figure 2 and Table 1 are wastewater disposal (wd), water injection into hot rock to develop enhanced geothermal systems (egs), hydraulic fracturing of oil and gas reservoirs to enhance production (frak), and injection for scientific studies of earthquakes (scientific). Most of the case histories in this study were selected because their earthquake sequences include events of unusually large magnitude in relation to the corresponding volumes of injected fluid.

As mentioned before, there have been only three reported earthquakes induced by permeability-enhancing treatments in unconventional oil and gas fields that were large enough to be felt at the surface. Of these, two are represented in Table 1 and Figure 2, BUK and GAR, with moment magnitudes of 2.3 and 3, respectively. The event of *M*3.6 recorded in the Horn River Basin, northern British Columbia [*BC Oil and Gas Commission*, 2012], is quite significant because of its unusually large magnitude for an earthquake induced by hydraulic fracturing, but it is not represented in Figure 2 because it was not possible to determine the injection volume responsible for this event with any confidence.

The smallest earthquake in Figure 2, *M*1.4, was induced by the injection of 200 m^3 of brine at a depth of 9 km in the KTB borehole [*Zoback and Harjes*, 1997; *Jost et al*., 1998]. This earthquake is included mostly to indicate how the KTB injection experiment relates to the other studies reviewed here.

The line in Figure 2 is based on assuming that a volume ΔV of liquid is injected into the crust and raises the pore pressure, thereby reducing the strength of the affected seismogenic rock mass. Earthquakes having a typical magnitude distribution are assumed to occur in response to the reduction in strength, as will be described in the next section.

Three of the earthquakes represented in Figure 2 and Table 1 merit further discussion with regard to how they are related to nearby injection activities. The first is the Painesville, Ohio, (POH) earthquake of January

Table 1. Maximum Seismic Moments M_0(Max) and Total Injected Volumes ΔV

Event	M_0(max) (N m)	ΔV (m^3)	Type[a]	M	Location
KTB [b]	1.43e11	200	scientific	1.4	eastern Bavaria, Germany
BUK[c]	3.2e12	4.17e3	frak	2.3	Bowland shale, UK
GAR[d]	3.5e13	1.75e4	frak	3.0	Garvin County, OK
STZ[e]	2.51e13	3.98e4	egs	2.9	Soultz, France
DFW[f]	8.9e13	2.82e5	wd	3.3	Dallas-Fort Worth Airport, TX
BAS[e]	1.41e14	1.15e4	egs	3.4	Basel, Switzerland
ASH[g]	2.82e14	6.17e4	wd	3.6	Ashtabula, OH, July, 1987
CBN[e]	3.98e14	2.0e4	egs	3.7	Cooper Basin, Australia
ASH[g]	8.0e14	3.4e5	wd	3.9	Ashtabula, OH, January 2001
YOH[h]	8.3e14	8.34e4	wd	4.0	Youngstown, OH
PBN[i]	3.16e15	3.287e6	wd	4.3	Paradox Valley, CO
RAT1[j]	4.5e15	4.26e5	wd	4.4	Raton Basin, CO, September 2001
GAK[k]	1.2e16	6.29e5	wd	4.7	Guy, AR
POH[l]	2.0e16	1.19e6	wd	4.8	Painesville, OH
RMA[m]	2.1e16	6.25e5	wd	4.85	Denver, CO
TTX[n]	2.21e16	9.91e5	wd	4.8	Timpson, TX
RAT2[o]	1.0e17	7.84e6	wd	5.3	Raton Basin, CO, August 2011
POK[p]	3.92e17	1.20e7	wd	5.7	Prague, OK

[a] frak = hydraulic fracturing; egs = enhanced geothermal system; wd = wastewater disposal.
[b] *Zoback and Harjes* [1997].
[c] *De Pater and Baisch* [2011].
[d] *Holland* [2013].
[e] *Majer et al.* [2007] and *Baisch et al.* [2006].
[f] *Frohlich et al.* [2011].
[g] *Seeber et al.* [2004] and *Nicholson and Wesson* [1990].
[h] *Ohio Department of Natural Resources* [2012] and *Kim* [2013].
[i] *Ake et al.* [2005].
[j] *Meremonte et al.* [2002].
[k] *Horton* [2012].
[l] *Nicholson et al.* [1988].
[m] *Herrmann et al.* [1981] and *Hsieh and Bredehoeft* [1981].
[n] *Frohlich et al.* [2013].
[o] J. L. Rubinstein et al. (manuscript submitted for publication, 2013).
[p] *Keranen et al.* [2013].

1986 [*Nicholson et al.*, 1988], the second is the Prague, Oklahoma, (POK) earthquake in November 2011 [*Keranen et al.*, 2013], and the third is the main shock (TTX) in May 2012 near Timpson, Texas [*Frohlich et al.*, 2013]. Because there are questions regarding their causes, I discuss their circumstances in more detail in a later section.

3. Upper Limit to Seismic Moment

An estimate of the upper bound seismic moment for a sequence of earthquakes induced by fluid injection into a geologic formation can be calculated based on the following assumptions:

1. The formation is either seismogenic or there is hydraulic communication between the injection interval and seismogenic regions of the crust. The seismogenic regions, which are often Precambrian crystalline basement formations, contain numerous preexisting faults, some of which are well oriented for failure in the ambient state of stress. [e.g., *Townend and Zoback*, 2000].
2. Before injection, faults in the vicinity of the injection wells that are well oriented for slip in the ambient stress field are stressed to within a seismic stress drop $\Delta\tau$ of failure.
3. The rock mass is fully saturated before injection begins.
4. The seismic response to injection is a *Gutenberg and Richter* [1954] earthquake distribution $\log N = a - bM$, where M is moment magnitude. In the following analysis, the commonly chosen b value of 1 is assumed, but I also describe the effects of different choices of b in section 5.
5. The induced earthquakes are localized to the region where the crust has been weakened due to fluid injection [*Hubbert and Rubey*, 1959]. This assumption seems plausible, but it is, nonetheless, difficult to prove that it always applies.

If a volume ΔV of liquid is injected into a fully saturated formation, then the average increase in pore pressure P is given by

$$\Delta P = \frac{3\lambda + 2G}{3}\frac{\Delta V}{V} \tag{1}$$

where V is the volume of the formation weakened by the injection and λ and G are Lame's elastic parameters, G being the modulus of rigidity. Equation (1) has implicit time dependence because the volume of injected fluid, ΔV, increases with time and also because of the increase in the affected volume, V, according to the physics of pore pressure diffusion. Aside from acknowledging that these time-dependent processes take place, however, I have not attempted any hydrological modeling [e.g., *Hsieh and Bredehoeft*, 1981; *Shapiro and Dinske*, 2009]. As will be seen, for the purposes of this study, the details of how or where the injected fluid diffuses through the rock mass can be neglected.

According to the effective stress law [*Hubbert and Rubey*, 1959], fault strength τ is given by

$$\tau = \tau_0 + \mu(\sigma_n - P) \tag{2}$$

where τ_0 is the cohesive strength, μ is the friction coefficient, and σ_n is the normal stress acting on the fault.

Assumption 2, above, states that any suitably oriented fault, or fault patch, within the seismogenic formation is within a seismic stress drop $\Delta\tau$ of failure; that is, if a long time has passed since the most recent earthquake, then the stress loading the fault would be close to the yield stress τ, whereas if an earthquake has just occurred, the fault would be at stress level $\tau - \Delta\tau$. Whether the tectonic setting is active or stable, there is always at least some secular strain accumulation that will continually increase the shear stress acting on a fault until reaching a limiting yield stress, at which point the fault slips thereby producing an earthquake with an associated stress drop. The initial shear stress acting on a fault well oriented for slip in the ambient stress field is in the range from $\tau_0 + \mu(\sigma_n - P)$ to $\tau_0 + \mu(\sigma_n - P) - \Delta\tau$ and so if the mean loading stress is at the center of this distribution, one would expect that, on average, an increase in pore pressure P given by

$$\Delta P = \frac{\Delta\tau}{2\mu} \tag{3}$$

would be sufficient to cause earthquakes.

According to *Kostrov* [1974, equation 3.10], the relationship between strain change $\Delta\varepsilon_{ij}$ and seismic moments for a distribution of earthquakes within a region of volume V is

$$\Delta\varepsilon_{ij} = \frac{1}{2GV}\Sigma M_{ij} \tag{4}$$

where M_{ij} are the moment tensor components of the earthquakes. This can be simplified to include only the deformation $\Delta\varepsilon$ that is consistent with the regional state of stress. Moreover, from Hooke's law, the shear strain change $\Delta\varepsilon$ can be converted into a stress drop using $\Delta\tau = 2G\Delta\varepsilon$ and so

$$\Delta\tau = \frac{1}{V}\Sigma M_0 \tag{5}$$

Then, combining equations (1), (3), and (5) gives

$$\Sigma M_0 = \frac{2\mu(3\lambda + 2G)}{3}\Delta V \tag{6}$$

In the course deriving equation (6), some important variables, V, ΔP, and $\Delta\tau$, have been eliminated by combining equations. I revisit these variables in the following section.

If, as is commonly assumed, $\lambda = G$, and if $\mu = 0.6$, a typical laboratory result for the coefficient of friction, then

$$\Sigma M_0 = 2G\Delta V \tag{7}$$

Equation (7) is similar to equation (8) of *McGarr* [1976], $\Sigma M_0 = KG|\Delta V|$, where $K \approx 1$, but the two equations differ by a factor of approximately 2. This discrepancy results from different assumptions in the two analyses.

The approach of *McGarr* [1976] was based on the idea that the volume change induces changes in the deviatoric stresses, which are relaxed by the induced earthquakes. That is, the seismic stress drops offset the shear stresses imposed by the volume change.

In contrast, the analysis here takes account of the likelihood that, on average, each fault patch is about half a seismic stress drop below the yield stress and so it only takes half as much stress change imposed by the volume change to induce seismic slip. That is, the injected fluid leads to pore pressure increase, which reduces the yield stress on average by half a seismic stress drop to the point at which it is equal to the loading stress.

To estimate the maximum moment $M_0(\max)$ in the distribution of earthquakes following the injection of ΔV of fluid, one can express the Gutenberg-Richter distribution in terms of seismic moment using

$$\log M_0 = 9.05 + 1.5M \tag{8}$$

where M_0 is in N m, adapted from the counterpart equation of *Hanks and Kanamori* [1979] for SI units. Equation (8), if combined with the magnitude-frequency relation $\log N = a - bM$, leads to

$$N = AM_0{}^{-B} \tag{9}$$

where $B = b/1.5$ and N is the number of earthquakes of seismic moment M_0, or greater, during the time interval under consideration. To evaluate A, I set the time interval to the total time since the start of injection and note that there is only one earthquake with the largest moment $M_0(\max)$. Thus,

$$N = M_0(\max)^B M_0{}^{-B} \tag{10}$$

The total earthquake deformation can be related to the distribution of seismic moments using

$$\Sigma M_0 = \int_0^{M_0(\max)} M_0 \left(-\frac{dN}{dM_0}\right) dM_0 = \frac{B}{1-B} M_0(\max) \tag{11}$$

Then, combining equations (6) and (11) gives

$$M_0(\max) = \frac{(1-B)}{B} \frac{2\mu(3\lambda + 2G)}{3} \Delta V \tag{12}$$

If $b = 1$, then $B = 2/3$. Moreover, if $\lambda = G$, as often assumed, and μ is assigned a typical laboratory value of 0.6, then

$$M_0(\max) = G\Delta V \tag{13}$$

Equation (13), with $G = 3e10$ Pa, is plotted in Figure 2 and appears to describe an upper bound to the data.

It is important to note that equations (6), (7), (12), and (13) are based on the assumption that all of the deformation induced by injecting a volume of fluid is seismic. Thus, these four equations should be taken as upper bounds. In most injection circumstances, the actual seismic outcome is observed to be much smaller than given by these equations for various reasons including (1) the formation experiencing the pore pressure increase deforms aseismically or (2) the permeability in the formation is so high that there is little or no pore pressure increase in response to injection.

It should also be emphasized that an important loophole in the derivation of the upper bound given by equation (13) is the possibility that the induced earthquakes may not be confined to the region experiencing an increase in pore pressure. As yet, this possibility cannot be dismissed and so it is an important source of uncertainty.

4. Pore Pressure Change, Stress Drop, and Volume

The analysis leading to equation (6) involved some important parameters, such as pore pressure change ΔP, that were eliminated in the course of finally arriving at a simple relation between an upper bound seismic moment and the total volume of injected fluid during the time leading up to the largest potential earthquake. These eliminated parameters can be estimated, as I now show.

First, seismic stress drops are routinely estimated and tend to be in the range 0.1 to 10 MPa [e.g., *Abercrombie*, 1995] for natural or induced earthquakes. Consider a typical stress drop $\Delta\tau = 3$ MPa, well within the range of estimated stress drops. Then from equation (3), with $\mu = 0.6$, the typical increase in pore pressure needed to cause seismic slip across a fault patch is $\Delta P = 2.5$ MPa, which is of the same order as the pore pressure increase of 3.2 MPa inferred by *Hsieh and Bredehoeft* [1981] for the Denver earthquakes.

From this pore pressure increase, equation (1) can be used to estimate the crustal volume V, which increases with time as the injected volume ΔV increases and also because of the effects of pore pressure diffusion away

from the injection interval. This pore pressure diffusion and other hydrological details have not been taken into account in any specific way here partly because this sort of information is difficult to obtain and generally model dependent. (*Shapiro et al*. [2011], for example, have analyzed magnitudes of earthquakes induced by fluid injection in terms of interactions between preexisting faults and the crustal volumes inferred to have experienced pore pressure increase.)

5. Influence of *B*

The moment frequency parameter B has a substantial influence on how the maximum moment is related to the volume of injected fluid. From equation (11) it is clear that B must be in the range between 0.5 and 1, assuming a moment distribution with a constant B value. If B is less than 0.5, then the cumulative seismic moment is less than the maximum moment, an impossible outcome, and if B is 1, the cumulative moment is infinitely large. Thus, $0.5 \le B < 1$. (This limit on B should not be taken as a comment on b values reported to be equal to or greater than 1.5. It is outside the scope of this report to discuss the possible reasons for this.)

The case history of the development of an enhanced geothermal system at Paralana, Australia [*Oye et al*., 2012; *Albaric et al*., 2013], provides a good example of the effect of B on the seismic moment distribution because of the comprehensive data set acquired there that was analyzed quite rigorously. As reported by *Albaric et al*. [2013], the injection of 3100 m^3 of water at a depth of about 3.6 km triggered more than 7000 recorded microearthquakes whose cumulative seismic moment is 8.7×10^{13} N m [*Albaric et al*., 2013, Figure 7]. This is close to what would be predicted using equation (6) with $G = 1.47 \times 10^{10}$ Pa (V. Oye, written communication, 2013) and assuming $\lambda = G$ and $\mu = 0.6$. That is, $\Sigma M_0 = \frac{2\mu(3\lambda+2G)}{3}\Delta V = 9.1 \times 10^{13}$Nm.

According to *Albaric et al*. [2013], $b = 1.32$ for the magnitude distribution of the microearthquakes and so $B = b/1.5 = 0.88$. From equation (12), the maximum seismic moment is predicted to be 1.24×10^{13} N m, equivalent to a moment magnitude of 2.7, which is not much higher than the observed maximum magnitude of 2.5 [*Albaric et al*., 2013]. This example shows that to the extent that B exceeds 2/3, the maximum seismic moment is reduced relative to what would be predicted from equation (13), M3.1, which would be the upper bound if $B = 2/3$.

6. Painesville, OH, Prague, OK, and Timpson, TX

As already noted, there are questions about the origins of the 1986 Painesville, OH, earthquakes, the 2011 Prague, OK, sequence, and the 2012 Timpson, TX, events. Here I review briefly the circumstances of these case histories in view of our present understanding of earthquakes induced by fluid injection.

6.1. Painesville, OH

This earthquake, assigned a magnitude $m_b = 5$, occurred on 31 January 1986 and was felt over a broad area according to *Nicholson et al*. [1988], who reported a very comprehensive study of this event. In addition to describing in detail this earthquake sequence, which included 13 aftershocks detected over the following 2.5 months, these authors also observed that there were three wastewater disposal wells in the vicinity that had injected nearly 1.2 million m^3 of wastewater into the basal aquifer at a depth of 1.8 km. The distance from the two nearly colocated wells, Calhio 1 and Calhio 2, which account for nearly all of the injected volume, to the main shock epicenter is about 12 km [*Nicholson et al*., 1988].

Nicholson et al. [1988] considered two hypotheses. The first proposes that the earthquakes were induced by the pore pressure increase due to injection that was channeled along the basal aquifer to a vertical fault where it was transmitted into the Precambrian granitic basement (e.g., Figure 1) where all of the earthquakes were located. The second hypothesis is a natural origin for these earthquakes.

Despite developing a plausible scenario relating large-volume wastewater injection to this earthquake sequence, *Nicholson et al*. [1988] were, nonetheless, unable to decide whether these Painesville earthquakes were natural or induced, partly because the injection began more than 10 years before these earthquakes and also because there were no in situ stress measurements in the hypocentral region; thus, it was not clear that the pore pressure changes transmitted into the hypocentral region were enough to induce the earthquakes. In particular, the authors were concerned that the state of stress in the Precambrian basement, where the

earthquakes were located, might be different and less favorable to fault slip than in the basal aquifer where the wastewater was injected.

Since 1988 there has been considerable progress in our understanding of the state of the seismogenic crust. Moreover, various aspects of seismicity induced by wastewater injection have been recognized in numerous case histories that lend additional support to the hypothesis that the Painesville, OH, earthquakes were induced, not natural:

1. There have been additional case histories of induced earthquakes attributed to wastewater injection in northeastern Ohio since 1988 at Ashtabula [*Seeber et al*., 2004] and Youngstown [*Kim*, 2013]. The Ashtabula case history has several features that tend to support the case that the Painesville earthquakes were induced. As will be described below, the larger Ashtabula event occurred 15 years after the start of injection and about 7 km from the injection well considered to have induced this earthquake [*Seeber et al*., 2004].
2. The hypocenters of these induced earthquakes are located in the Precambrian basement [*Seeber et al*., 2004; *Kim*, 2013]
3. Although the 12 km distance between the two high-volume injection wells and the Painesville earthquakes could be taken as evidence favoring a natural origin, there is some precedence for earthquakes being induced at comparable distances from injection wells. Most of the Guy, Arkansas, earthquakes, for instance, were located in the basement at distances ranging up to between 10 and 15 km from the two injection wells implicated in this sequence [*Horton*, 2012].
4. More recent reports of induced earthquakes [e.g., *Keranen et al*., 2013; J. L. Rubinstein et al., manuscript submitted for publication, 2013] include examples for which the time between the start of injection and when the first earthquakes were noticed was quite long, sometimes of the order of 10 years.
5. In situ stress measurements in deep boreholes worldwide support the notion that basement formations tend to be in a near-critical state of stress [e.g., *Townend and Zoback*, 2000].

In summary, based on these various additions during the past 25 years to our understanding of the ambient state of the seismogenic crust and of earthquakes induced by deep fluid injection, it currently seems more likely that the Painesville earthquakes were induced than it may have to [*Nicholson et al*. 1988].

6.2. Prague, Oklahoma

The *M*5.7 main shock is of exceptional importance in the central and eastern United States because it is the second largest earthquake that has been recorded in this vast region. Because of its substantial role in assessing the seismic hazard, especially in central Oklahoma, there is an urgent need to understand its origin. There were three earthquakes of *M*5 or greater in the Prague sequence, a foreshock of *M*5 on 5 November, the *M*5.7 main shock on 6 November, and an aftershock of *M*5 on 8 November [*Keranen et al*., 2013]. Currently, there are at least three hypotheses for this earthquake sequence:

1. The Prague earthquakes are of natural origin [*Keller and Holland*, 2013].
2. The *M*5 foreshock was triggered by pore pressure increase due to wastewater injected from two wells near the northeast end of the epicentral zone. This foreshock, in turn, increased the Coulomb stress [e.g., *Stein and Lisowski*, 1983] acting on preexisting faults so as to trigger the *M*5.7 main shock, which was followed by the *M*5 aftershock and numerous additional aftershocks of smaller magnitude [*Keranen et al*., 2013].
3. The earthquake sequence was the result of approximately 1.2e7 m^3 of wastewater injected in the vicinity of the epicentral zone mostly from five high-volume injection wells. The seismic moment of the main shock is consistent with this hypothesis in terms of equation (13) and Figure 2.

As shown by *Ellsworth et al*. [2012], and more recently by *Ellsworth* [2013] and W. L. Ellsworth et al. (manuscript in preparation, 2013), the seismicity in central Oklahoma has increased dramatically starting in 2009, an increase that is inconsistent with any natural processes that are likely to occur in this geologically stable area. For central Oklahoma, it appears more likely that the remarkable increase in seismicity is the result of deep injection of wastewater associated with the rapid growth of oil and gas production, enabled by new technologies, that has taken place in recent years.

But, even if the increase in seismicity in central Oklahoma is not due to natural tectonic causes, this is not necessarily a valid argument that the Prague earthquake sequence is due to oil and gas activities [*Keller and*

Table 2. Five High-Volume Injection Wells in Epicentral Region of Prague, OK, Earthquakes Plus Stasta Wells 1 and 2[a]

Well	Start Year	ΔV[b] (10^6 m^3)	Latitude (deg)	Longitude (deg)
Wilzetta-1	1999	3.89	35.558	−96.738
Turner-1	2004	2.57	35.443	−96.726
Jesse-1	2003	2.31	35.427	−96.702
Howard-1	2008	1.44	35.422	−96.754
Mazkoori-1	2000	0.99	35.541	−96.751
Stasta-1	1993	0.05	35.560	−96.750
Stasta-2	2006	0.05	35.562	−96.750

[a]These data were provided by Austin Holland of the Oklahoma Geological Survey.
[b]Volumes include injection up to the end of 2010.

Holland, 2013]. If hypothesis 1 is correct, then the point labeled POK should be removed from Figure 2 and Table 1.

With regard to hypothesis 2, *Keranen et al*. [2013] stated that the Prague earthquakes are "potentially induced" by wastewater injection. Their argument focused on injection of nearly 100,000 m^3 of wastewater down two nearly colocated wells, Stasta 1 and Stasta 2 (Table 2). These two wells, according to the scenario proposed by *Keranen et al*. [2013] raised the pore pressure within a fault zone extending southwestward from the wells and thereby triggered the *M*5 foreshock, which, in turn, triggered the *M*5.7 main shock, through Coulomb stress transfer [e.g., *Stein and Lisowski*, 1983].

In the context of the other case histories reviewed here (Figure 2 and Table 1), it seems somewhat unlikely that the injection of about 100,000 m^3 of wastewater down the two Stasta wells could trigger the *M*5 foreshock of 5 November. According to equation (13), with $G = 3 \times 10^{10}$ Pa, the upper bound seismic moment would be 3×10^{15} N m, whereas the two moment estimates for this foreshock listed on the National Earthquake Information Center website of the U.S. Geological Survey are 2×10^{16} N m and 3.6×10^{16} N m; thus, the reported seismic moments of the large foreshock are about an order of magnitude greater than the upper bound inferred from the injected volume. That is, a relatively small volume of injected wastewater from the two Stasta wells gave rise to a disproportionately large earthquake response. Needless to say, this could be construed as a counterexample to the upper bound given by equation (13), but, as will be argued next, hypothesis 2 involves neglecting the likely effects of some injection wells in the epicentral area shown in *Keranen et al*. [2013, Figure 1] that injected vastly greater volumes of wastewater in comparison to what was injected by Stasta 1 and 2 (Table 2).

Hypothesis 3 is favored here partly because the Prague earthquake sequence seems to share attributes with other case histories of earthquakes induced by deep injection of wastewater [e.g., *Horton*, 2012]. The zone of earthquakes is in a region where exceptionally large volumes of wastewater have been injected into the Arbuckle formation, a basal dolomitic limestone aquifer [*Keranen et al*., 2013] that is attractive for fluid injection because of its high porosity and permeability. This aquifer is well suited to transmit pore pressure increases to the Wilzetta faults in the zone of epicenters and then into the Precambrian basement (Figure 1), where most of the Prague earthquakes were located [*Keranen et al*., 2013, Figure 1]. The total volume injected down the wells in the epicentral region [*Keranen et al*., 2013, Figure 1] up to the end of 2010 is 1.2e7 m^3, which, according to equations (8) and (13), is consistent with a maximum moment magnitude of 5.7. There were five wells that account for 93% of this injected volume (Table 2). Wilzetta-1 accounts for 32% of the total volume and is located at the northeast end of the epicenters, quite close to the Stasta 1 and 2 wells. Mazkoori-1, located within the zone of epicenters, accounts for 8% of the total volume. The other three high-volume wells that account for much of the rest of the total volume (Table 2) are at distances of 10 to 12 km southeast of the *M*5.7 main shock epicenter. *Keranen et al*. [2013, Figure 1] show an isolated cluster of 11 aftershocks located in the vicinity of the three high-volume wells to the southeast of the main epicentral zone, Turner-1, Jesse-1, and Howard-1. The location of this cluster, as well as several other aftershock epicenters further to the northwest toward the main shock epicenter, provides support to the proposal that there was hydraulic communication between these three wells and the faults that ruptured during the *M*5.7 main shock.

Note that I do not claim to have demonstrated that either of the first two hypotheses listed above can be ruled out. My only intention here is to argue that the third hypothesis is also plausible. More research is needed to eliminate any of these hypotheses.

6.3. Timpson, Texas

This is another case history for which there are multiple injection wells in the epicentral region. As noted by *Frohlich et al*. [2013], there were two high-volume injection wells, labeled "north" and "south", within 3 km of the intensity VII region of the 17 May 2012 Timpson *M*4.8 main shock and two lower volume wells somewhat

further away from the region of highest intensity. The fault plane defined by the best located hypocenters dips southeastward; the upper edge of the plane is close to the injection interval of the "north" well as viewed in cross section [*Frohlich et al*., 2013, Figure 6]. Thus, the "north" well appears to have been the most likely to have increased the pore pressure within the fault zone imaged by the well-located hypocenters; in contrast, neither the "south" well nor the two smaller-volume wells appear to be related to the hypocenters in any obvious way.

Accordingly, for purposes of the analysis here, the total volume of wastewater injected down the "north" well up to the time of the main shock on 17 May 2012, about 0.99 million m^3 [*Frohlich et al*., 2013, Figure 11], is used to relate the injection activities to the maximum seismic moment for the Timpson sequence (Figure 2 and Table 1).

7. Discussion

7.1. Time-Dependent Growth of M_0(max)

Even though equation (13) does not have any explicit dependence on time or injection rate, there is, nonetheless, the time dependence of the total volume of injected fluid, which increases with time as long as injection continues. There is also time dependence imposed by hydrological factors that control the diffusion of pore pressure away from the injection interval [e.g., *Hsieh and Bredehoeft*, 1981]. Accordingly, one expects the upper bound magnitude or seismic moment to increase with a time dependence that can be quite irregular, exemplified by some of the case histories reviewed here. The following two examples illustrate how the upper bound seismic moment increases with time, but these examples, as well as the others, demonstrate that taking account of the factors that control this time dependence in a detailed way is a formidable challenge.

As described by *Seeber et al*. [2004], the two Ashtabula, OH, main shocks (Table 1), *M*3.6 in 1987 and *M*3.9 in 2001, were located near a wastewater disposal well that was active from 1986 to 1993. These two main shocks (Figure 2 and Table 2) have moments that have evidently been controlled by the total volume of wastewater injected before they occurred. In more detail [see *Seeber et al*., 2004, Figure 2], the nearby wastewater disposal well first induced the *M*3.6 event, whose epicenter was about 1 km southwest of the well. The *M*3.9 epicenter was located between 6.5 and 7 km southwest of the disposal well and occurred about 7 years after the injection activity had stopped. Thus, it appears that the pore pressure increase due to wastewater injected from 1986 to 1993 migrated southwestward from the injection point and finally induced the *M*3.9 earthquake in January 2001. In addition to illustrating the idea that the maximum seismic moment increases with time and is limited according to the total injection volume, this case history also shows that the time histories of injection and the occurrence of larger-magnitude-induced earthquakes can be quite different, depending most likely on hydrological factors that influence how pore pressure effects migrate through the rock mass [e.g., *Hsieh and Bredehoeft*, 1981]. That is, there is no reason to expect that the occurrence of the largest earthquakes induced by fluid injection is well correlated with the time history of injection.

The sequence of earthquakes in southern Colorado that began near the town of Trinidad in 2001 [*Meremonte et al*., 2002] also provides evidence that maximum magnitudes of induced earthquakes increase with time and are limited by the injected volume. The initial sequence of earthquakes, August to October 2001, was centered closely around the Wild Boar injection well that had been active since April 2000. The largest event of this swarm, *M*4.4 (Table 1 and RAT1 in Figure 2), occurred in September 2001 [*Meremonte et al*., 2002] when about 426,000 m^3 of wastewater had been injected. The well-located hypocenters and focal mechanisms indicated a previously unknown normal fault extending about 7 km along its northeast strike and dipping toward the southeast.

Ten years later, in response to the 23 August 2011 *M*5.3 earthquake (Table 1 and Figure 2), Mark Meremonte and his U.S. Geological Survey colleagues deployed a small network of portable stations so that events in this sequence could be precisely located. The well-located hypocenters defined an extension of the fault zone of the 2001 swarm about 12 km toward the southwest (J. L. Rubinstein et al., manuscript submitted for publication, 2013). Near the southwest end of the extended fault zone there are two nearly colocated wells, VPRC-14 and VPRC-39, which together had injected almost 5 million m^3 of wastewater by 23 August 2011 (J. L. Rubinstein et al., manuscript submitted for publication, 2013). From the distribution of earthquakes, it appears that this

sequence was induced by a total of 7.8 million m^3 of wastewater along the newly imaged fault zone (J. L. Rubinstein et al., manuscript submitted for publication, 2013) including 2.8 million m^3 from the Wild Boar well at the northeast end of the fault zone that had continued injection following the 2001 swarm (Table 1 and RAT2 in Figure 2).

In summary, it is clear from these and other case histories that taking time-dependent effects into account in any detail would be truly challenging, partly because of an incomplete understanding of the hydrological response of the crust to injection.

7.2. Can Seismic Moments or Magnitudes Be Capped?

The data plotted in Figure 2 suggest that it may be possible to limit seismic moments or magnitudes based on the total volume of injected fluid. If so, this is a useful result, especially for purposes of attempting to estimate the contribution of induced earthquakes to the total seismic hazard. That is, for a planned injection activity involving a single well or a set of wells, one could use equation (12) or (13) to estimate an upper bound seismic moment for the project based on the total volume to be injected. But this upper bound has uncertainty.

As noted before, the main source of uncertainty in using equations (12) or (13) to estimate the worst case earthquake is the assumption that the seismic fault slip in response to injection is limited to the region experiencing a pore pressure increase. Although the evidence summarized in Figure 2 tends to support an upper bound given by equation (13), it is probably most realistic to consider it a plausible, but somewhat uncertain, upper bound.

8. Conclusions

In brief summary, the main conclusions of this study are as follows:

1. So far, it appears that maximum seismic moments are limited based on the total volume injected in the environs of the induced earthquakes according to equation (13).
2. An upper bound to seismic moment for a given fluid injection activity is estimated as $M_0(\max) = G\Delta V$ based on the assumption that fluid is injected into a saturated formation that deforms seismically with an earthquake distribution having a Gutenberg-Richter magnitude-frequency distribution with a *b* value of 1. A higher *b* value would result in a lower maximum moment (equation (12)).
3. This upper bound increases with time as long as the corresponding injection activities continue.
4. The cumulative seismic moment is roughly $\sum M_0 = 2G\Delta V$, which is about twice the cumulative moment from a corresponding equation developed by *McGarr* [1976]. The more general version is $\sum M_0 = \frac{2\mu(3\lambda+2G)}{3}\Delta V$.
5. The possibility that injection induces an earthquake that is larger than the upper bound of equation (13) cannot be ruled out because it is difficult to prove that an induced earthquake will necessarily be confined to the region experiencing an increase in pore pressure. At this time, however, the only reported [*Keranen et al*., 2013] counterexample to equation (13) is equivocal in that there is also a plausible interpretation of the Prague, Oklahoma, earthquake sequence that is consistent with equation (13) (Figure 2 and Table 2); additionally, the sequence might be natural [*Keller and Holland*, 2013].

Acknowledgments
I thank Justin Rubinstein, Keith Knudsen, Gail Atkinson, and Cliff Frohlich for their insightful reviews that improved this manuscript. I am grateful to Volker Oye for his input regarding the seismicity induced during the enhanced geothermal systems Project at Paralana, Australia. Thanks also to Austin Holland, of the Oklahoma Geological Survey, for providing the wastewater injection information for the aftershock region of the Prague, Oklahoma, earthquake. Joe Fletcher and Justin Rubinstein helped with the preparation of Figure 2.

References

Abercrombie, R. E. (1995), Earthquake source scaling relationships from −1 to 5 M_L using seismograms recorded at 2.5-km depth, *J. Geophys. Res.*, *100*, 24,015–24,036.
Ake, J., K. Mahrer, D. O'Connell, and L. Block (2005), Deep injection and closely monitored induced seismicity at Paradox Valley, Colorado, *Bull. Seismol. Soc. Am.*, *95*, 664–683.
Albaric, J., V. Oye, N. Langet, M. Hastings, I. Lecomte, K. Iranpour, M. Messeiller, and P. Reid (2013), Monitoring of induced seismicity during the first geothermal reservoir stimulation at Paralana, Australia, *Geothermics*, doi:10.1016/j.geothermics.2013.10.013.
Baisch, S., R. Weidler, R. Voros, D. Wyborn, and L. de Graaf (2006), Induced seismicity during the stimulation of a geothermal HFR reservoir in the Cooper Basin, Australia, *Bull. Seismol. Soc. Am.*, *96*, 2242–2256.
BC Oil and Gas Commission (2012), Investigation of observed seismicity in the Horn River Basin, 29 p.
Chapman, M. C. (2013), On the rupture process of the 23 August 2011 Virginia earthquake, *Bull. Seismol. Soc. Am.*, *103*, 613–628.
Davis, S. D., and W. D. Pennington (1989), Induced seismic deformation in the Cogdell oil field of west Texas, *Bull. Seismol. Soc. Am.*, *79*, 1477–1495.
De Pater, C. J., and S. Baisch (2011), Geomechanical study of Bowland Shale seismicity, Cuadrilla Resources Ltd., 57 p.
Ellsworth, W. L. (2013), Injection-induced earthquakes, *Science*, *341*, 142.
Ellsworth, W. L., S. H. Hickman, A. Llenos, A. McGarr, A. J. Michael, and J. L. Rubinstein (2012), Are seismicity rate changes in the midcontinent natural or manmade?, *Abstract, Seismol. Res. Lett.*, *82*, 403.

Frohlich, C. (2012), Two-year survey comparing earthquake activity and injection-well locations in the Barnett Shale, Texas, *Proc. Natl. Acad. Sci. U. S. A.*, *34*, 1–5, doi:10.1073/pnas.1207728109.
Frohlich, C., and M. Brunt (2013), Two-year survey of earthquakes and injection/production wells in the Eagle Ford Shale, Texas, prior to the M_W4.8 20 October 2011 earthquake, *Earth Planet. Sci. Lett.*, *379*, 56–63, doi:10.1016/j.epsl.2013.07.025.
Frohlich, C., C. Hayward, B. Stump, and E. Potter (2011), The Dallas-Fort Worth earthquake sequence: October 2008 through May 2009, *Bull. Seismol. Soc. Am.*, *101*, 327–340.
Frohlich, C., W. Ellsworth, W. A. Brown, M. Brunt, J. Luetgert, T. MacDonald, and S. Walter (2013), The 17 May 2012 M4.8 earthquake near Timpson, east Texas: An event possibly triggered by fluid injection, *J. Geophys. Res. Solid Earth*, doi:10.1002/2013JB010755, in press.
Gan, W., and C. Frohlich (2013), Gas injection may have triggered earthquakes in the Cogdell oil field, Texas, *Proc. Natl. Acad. Sci. U. S. A.*, *110*(47), 18,786–18,791, doi:10.1073/pnas.1311316110.
Gutenberg, B., and C. Richter (1954), *Seismicity of the Earth*, 2nd ed., pp. 16–25, Princeton Univ. Press, Princeton, N.J.
Hanks, T., and H. Kanamori (1979), A moment magnitude scale, *J. Geophys. Res.*, *84*, 2348–2350.
Healy, J. H., W. W. Rubey, D. T. Griggs, and C. B. Raleigh (1968), The Denver earthquakes, *Science*, *161*, 1301–1310.
Herrmann, R. B., S.-K. Park, and C.-Y. Wang (1981), The Denver earthquakes of 1967–1968, *Bull. Seismol. Soc. Am.*, *71*, 731–745.
Holland, A. (2013), Earthquakes triggered by hydraulic fracturing in south-central Oklahoma, *Bull. Seismol. Soc. Am.*, *103*, 1784–1792.
Horton, S. (2012), Disposal of hydrofracking waste fluid by injection into subsurface aquifers triggers earthquake swarm in central Arkansas with potential for damaging earthquake, *Seismol. Res. Lett.*, *83*, 250–260.
Hsieh, P. A., and J. D. Bredehoeft (1981), A reservoir analysis of the Denver earthquakes: A case of induced seismicity, *J. Geophys. Res.*, *86*, 903–920.
Hubbert, M. K., and W. W. Rubey (1959), Role of fluid pressure in mechanics of overthrust faulting: 1. Mechanics of fluid-filled porous solids and its application to overthrust faulting, *Geol. Soc. Am. Bull.*, *70*, 115–166.
Jost, M. L., T. Busselberg, O. Jost, and H.-P. Harjes (1998), Source parameters of injection-induced microearthquakes at 9 km depth at the KTB deep drilling site, Germany, *Bull. Seismol. Soc. Am.*, *88*, 815–832.
Keller, G. R., and A. Holland (2013), Oklahoma Geological Survey evaluation of the Prague earthquake sequence of 2011. [Available at http://www.ogs.ou.edu/earthquakes/OGS_PragueStatement201303.pdf.]
Keranen, K. M., H. M. Savage, G. A. Abers, and E. S. Cochran (2013), Potentially induced earthquakes in Oklahoma, USA: Links between wastewater injection and the 2011 M_w 5.7 earthquake sequence, *Geology*, G34045.1, doi:10.1130/G34045.1.
Kim, W.-Y. (2013), Induced seismicity associated with fluid injection into a deep well in Youngstown, Ohio, *J. Geophys. Res. Solid Earth*, *118*, 3506–3518, doi:10.1002/jgrb.50247.
Kostrov, B. V. (1974), Seismic moment and energy of earthquakes, and seismic flow of rock, U.S.S.R. Academy of Sciences Izvestiya, *Phys. Solid Earth*, *1*, 23–44.
Majer, E., R. Baria, M. Stark, S. Oates, J. Bommer, B. Smith, and H. Asanuma (2007), Induced seismicity associated with enhanced geothermal systems, *Geothermics*, *36*, 185–222.
McGarr, A. (1976), Seismic moments and volume changes, *J. Geophys. Res.*, *81*, 1487–1494.
McGarr, A., D. Simpson, and L. Seeber (2002), Case histories of induced and triggered seismicity, in *International Handbook of Earthquake and Engineering Seismology*, vol. 81A, pp. 647–661, Academic Press, San Francisco, Calif.
Meremonte, M. E., J. C. Lahr, A. d. Frankel, J. W. Dewey, A. J. Crone, D. E. Overturf, D. L. Carver, and W. T. Bice (2002), Investigation of an earthquake swarm near Trinidad, Colorado, August-October 2001, *Open-File Report* 02-0073, U. S. Geological Survey, 32 p.
National Research Council (2013), *Induced Seismicity Potential in Energy Technologies*, 225 p., National Academies Press, Washington, D. C. [Available at http://dels.nas.edu/Report/Induced-Seismicity-Potential-Energy-Technologies/13355.]
Nicholson, C., and R. L. Wesson (1990), *Earthquake Hazard Associated With Deep Well Injection: A Report to the U.S. Environmental Protection Agency*, U.S. Geological Survey Bulletin 1951, 74 p., United States Government Printing Office, Washington, D. C.
Nicholson, C., E. Roeloffs, and R. L. Wesson (1988), The northeastern Ohio earthquake of 31 January 1986: Was it induced?, *Bull. Seismol. Soc. Am.*, *78*, 188–217.
Ohio Department of Natural Resources (2012), Preliminary report on the Northstar 1 class II injection well and the seismic events in the Youngstown, Ohio area, 23 p.
Oye, V., J. Albaric, N. Langer, M. Hasting, I. Lecomte, M. Messeiller, and P. Reid (2012), Microseismic monitoring of the hydraulic stimulation at the Paralana enhanced geothermal system, South Australia, *First Break*, *30*, 91–95.
Pennington, W. D., S. D. Davis, S. M. Carlson, J. DuPree, and T. E. Ewing (1986), The evolution of seismic barriers and asperities caused by the depressuring of fault planes in oil and gas fields of South Texas, *Bull. Seismol. Soc. Am.*, *76*, 939–948.
Raleigh, C. B., J. H. Healy, and J. D. Bredehoeft (1976), An experiment in earthquake control at Rangely, Colorado, *Science*, *91*, 1230–1237.
Seeber, L., J. Armbruster, and W.-Y. Kim (2004), A fluid-injection-triggered earthquake sequence in Ashtabula, Ohio: Implications for seismogenesis in stable continental regions, *Bull. Seismol. Soc. Am.*, *94*, 76–87.
Shapiro, S. A., and C. Dinske (2009), Scaling of seismicity induced by nonlinear fluid-rock interaction, *J. Geophys. Res.*, *114*, B09307, doi:10.1029/2008JB006145.
Shapiro, S. A., O. S. Kruger, C. Dinske, and C. Langenbruch (2011), Magnitudes of induced earthquakes and geometric scales of fluid-stimulated rock volumes, *Geophysics*, *76*, WC55–WC63, doi:10.1190/GEO2010-0349.1.
Stein, R. S., and M. Lisowski (1983), The 1979 Homestead Valley earthquake sequence, California: Control of aftershock and postseismic deformation, *J. Geophys. Res.*, *88*, 6477–6490.
Townend, J., and M. D. Zoback (2000), How faulting keeps the crust strong, *Geology*, *28*, 399–402.
Zoback, M. D., and H.-P. Harjes (1997), Injection-induced earthquakes and crustal stress at 9 km depth at the KTB deep drilling site, Germany, *J. Geophys. Res.*, *102*, 18,477–18,491.